GLOBAL CHANGE: THE SIGNAL IN TROPICAL OCEAN TEMPERATURE AND SAHEL RAINFALL

With 11 figures and 1 table

STEFAN HASTENRATH

Zusammenfassung: Global Change-Signale in den Oberflächentemperaturen tropischer Meere und den Sahel-Niederschlägen

Aus den hydrometeorologischen Meßserien im randsaharischen Westafrika sowie Schiffsbeobachtungen der Oberflächentemperaturen tropischer Meere werden verschiedene Regime von Klimatrends seit dem Beginn unseres Jahrhunderts abgeleitet. Während der ersten Hälfte des Jahrhunderts schwankte der Abfluß des Senegal-Flusses in nahezu zyklischer Art, mit Niedrigständen in den zehner und frühen vierziger Jahren und Hochständen in den zwanziger und fünfziger Jahren. Die Oberflächentemperaturen im tropischen Nordatlantik zeichneten sich durch ähnliche Extreme aus, jedoch wurde die Periode 1900–1950 in mehreren Bereichen der tropischen Meere sowohl im Nordsommer wie im Winter durch einen augenscheinlichen Trend zur Erwärmung beherrscht. Die Daten sind zwar von einem Wechsel der Beobachtungstechniken beeinflußt, doch ist dieser Erwärmungstrend teilweise als real anzusehen. 1950–1980 wurde das randsaharische Westafrika von einer fortschreitend verstärkten Dürre betroffen, wie in den Niederschlags- und Abflußwerten deutlich wird. Damit ging ein signifikanter Abkühlungstrend im tropischen Nordatlantik einher (besonders ausgeprägt während des nordhemisphärischen Hochsommers Juli-August), während der tropische Südatlantik und Indik sich weiterhin erwärmten. Seit 1980 erleben wir die Entwicklung eines Regimes, das sich von den vorangegangenen drei Jahrzehnten deutlich unterscheidet: die Saheldürre zeigt eine Abschwächung, wie in den Niederschlägen deutlicher wird als in den Abflußwerten; die äquatoriale Windkonvergenz nimmt während des Nordsommers offenbar eine weiter nördlich gelegene Position ein; im tropischen Nordatlantik ist die Abkühlung von einer signifikanten Erwärmung im Nordsommer abgelöst worden, während sich der Erwärmungstrend im Südatlantik und Indik verstärkt hat. Im äquatorialen Pazifik ist der Trend der Oberflächentemperaturen weniger ausgeprägt. Zusammenfassend lassen sich im tropischen Atlantik und afrikanischen Sektor drei Hauptregime von Klimatrends unterscheiden, die etwa die Zeitabschnitte 1900–1950, 1950–1980 und ab 1980 umfassen. Die Entwicklungen während der jüngsten Dekade verdienen weitere Beachtung im Hinblick auf den Treibhauseffekt und Global Change.

1 Introduction

The growing concern about the greenhouse effect and global warming has led to a major effort at the international level to compare model expectations with observational evidence (HOUGHTON et al. 1990), and there is an incipient appreciation for the relevance of these processes to the formulation of public policy (GORE 1992). It is being increasingly realized that atmosphere, oceans, cryosphere, and land surface conditions, all merit attention in this context, and it has been pointed out (WOLTER a. HASTENRATH 1989) that, over recent decades, some parts of the world definitely cooled while other regions may have warmed; observational evidence seems insufficient to ascertain whether this mosaic of warming and cooling trends may have amounted to a temperature increase for the globe as a whole. Within the tropics, the sensitive climatic transition zone of the West African Sahel stands out as a region in which rainfall has progressively decreased from the late 1940's into the 1980's (LAMB 1985, LAMB a. PEPPLER 1991), and this was accompanied by a shift in the surface wind pattern (HASTENRATH 1990 a) and significant temperature trends in the tropical Atlantic and Indian Oceans (WOLTER a. HASTENRATH 1989). In a similar vein, there are indications for an accelerated shrinkage of tropical glaciers in the course of very recent decades (HASTENRATH a. KRUSS 1992). Accordingly, there is good reason to ascertain the changes of the tropical atmosphere-ocean-land system since the 1980's. As a contribution to that end, the present paper examines the sea surface temperature (SST) and rainfall trends in the course of this century, with a focus on Subsaharan West Africa and the tropical Atlantic and Indian Oceans.

2 Background

The annual cycle of circulation and climate over the tropical Atlantic and Indian Oceans is comprehensively documented elsewhere (HASTENRATH a. LAMB 1977, 1979; HASTENRATH 1991, p. 169–175) and a brief summary must suffice here. Rainfall over Subsaharan West Africa (Figs. 1 a. 2) is associated with the seasonal displacement of the Intertropical Convergence Zone, which migrates northward along with a band of highest SST to reach a northernmost location at the height of the boreal summer. The lower-

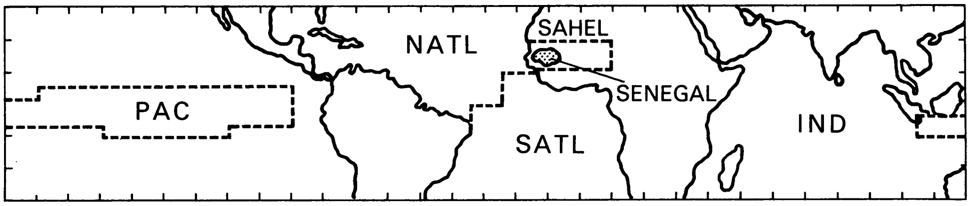

Fig. 1: Orientation map showing domain of rainfall index SAHEL, river catchment of SENEGAL, and areas for which the sea surface temperature (SST) indices NATL, SATL, IND, and PAC, were compiled

Orientierungskarte: Lage des Gebietes für den Niederschlagsindex SAHEL, Einzugsgebiet des Senegal-Flusses (SENEGAL) sowie Meeresflächen, für welche die Oberflächentemperatur-Indizes (SST: NATL, SATL, IND, PAC) zusammengestellt wurden

tropospheric structure over West Africa at this time of the year is illustrated in Fig. 2 (GERMAIN 1968), which indicates the most intense weather activity well to the South of the surface wind discontinuity. In this context, Fig. 3 (DETTWILLER 1965) depicts the steep meridional rainfall gradients between the Sahara Desert and the rainforest regions along the Gulf of Guinea, corresponding for the year as a whole to about 160 mm for 100 km of meridional distance.

Work at the University of Wisconsin since the mid 1970's (LAMB 1978a, b; HASTENRATH 1978) revealed that the interannual variability of rainfall in Subsaharan West Africa is associated with distinct anomalies of lower-tropospheric circulation and SST in the tropical Atlantic. Later papers (FOLLAND et al. 1986; BHATT 1989) also pointed out an affinity with SST in the Western Indian Ocean. Fig. 4 shows the considerable year-to-year variations of rainfall in the Sahel during the past half-century. The SST distribution in the tropical Atlantic characteristic of extreme rainfall years in the Sahel (HASTENRATH 1984) reproduced in Fig. 5, shows for WET as compared to DRY events anomously warm/cold waters in the tropical North/South Atlantic. Regarding the Western Indian Ocean, FOLLAND et al. (1986) and BHATT (1989) find anomously warm surface waters accompanying dry conditions in Subsaharan Africa.

A striking feature of Sahel rainfall during 1948–83 highlighted in Fig. 4 is the drastic downward trend. As seen from Fig. 6 (HASTENRATH 1990a) this was accompanied by a southward displacement of the surface wind discontinuity by about 200 km. In the light of Figs. 2 and 3, a similar southward shift of the isohyets should be envisaged. Given the steep meri-

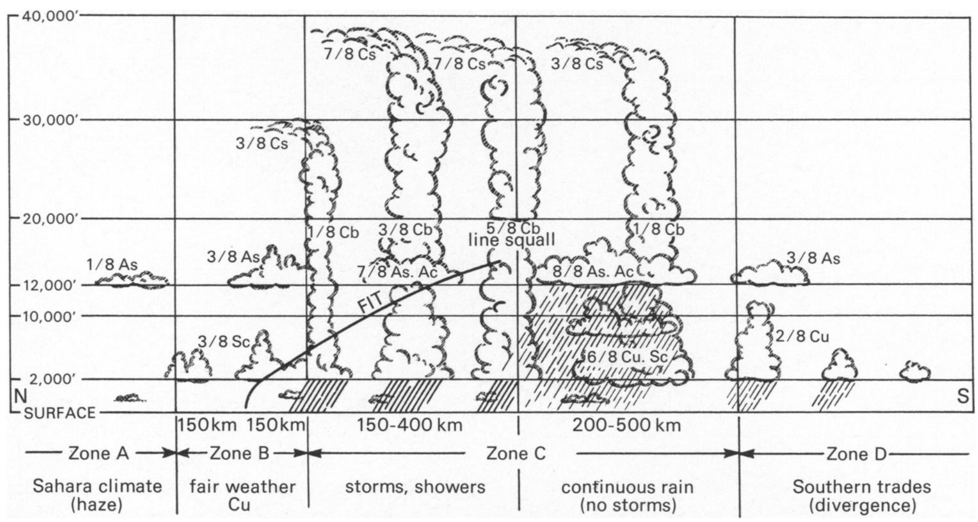

Fig. 2: Meridional-vertical transect across the Intertropical Convergence Zone over West Africa along about 0° longitude in boreal summer
Source: GERMAIN 1968

Meridionales Vertikalprofil der innertropischen Konvergenzzone über Westafrika etwa entlang des 0°-Meridians im Nordsommer

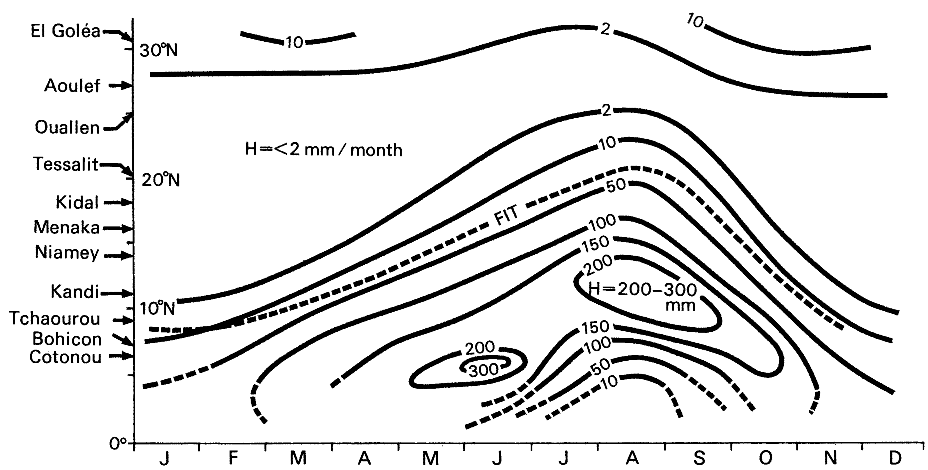

Fig. 3: Variation of monthly rainfall totals (in mm) with latitude and time of year along about 0–5° E longitude. Dashed line denotes surface position of discontinuity
Source: Dettwiller 1965

Wandel der monatlichen Niederschlagssummen (in mm) in Abhängigkeit von der Breitenlage und Jahreszeit im Profilstreifen 0–5° E

dional precipitation gradient across the region, this corresponds to a concomitant decrease of annual rainfall of nearly 300 mm, broadly in accordance with the observed change shown in Fig. 4. Whether the widely publicized southward expansion of the Sahara Desert should be regarded primarily as a cause of the demonstrated large-scale circulation changes or rather a consequence of it, remains an open issue (Hastenrath 1990b). In this spirit it should also be noted that after years of public debate on this issue a systematic effort on the in-situ monitoring of surface conditions in the sensitive transition zone between the desert in the North and the rainforest in the South is still lacking.

In the context of the drastic changes of Sahel rainfall and wind confluence documented in Figs. 4 and 6, the trends of SST in the tropical oceans during 1948–83 (Wolter a. Hastenrath 1989) are of interest. Fig. 7 demonstrates that concomitant which the aggravating drought in the Sahel, the tropical North

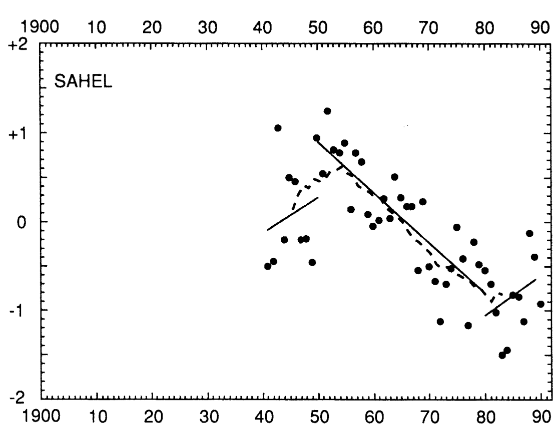

Fig. 4: Time series plot of rainfall index series SAHEL (ref. Fig. 1 for location). Heavy dots denote individual years, dashed line eleven-year running means, and solid line trends for the intervals 1950–80 and 1980–90

Darstellung der Zeitreihen des Niederschlagsindex SAHEL

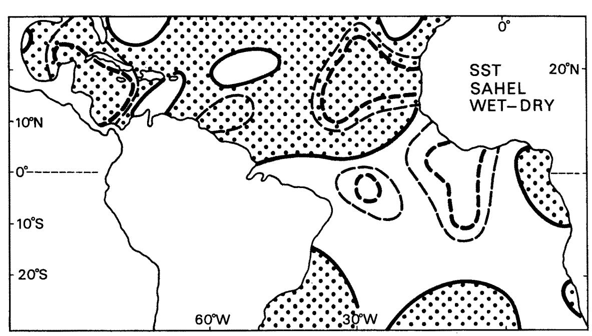

Fig. 5: Map of July–August sea surface temperature during WET (1943, 50, 52, 54, 55, 57) minus DRY (1941, 44, 68, 70, 71, 72) years in Subsaharan Africa. Dot raster indicates positive areas, domains significant at the 5 and 10% levels are enclosed, respectively, by heavy and thin broken lines
Source: Hastenrath 1984

Karte der Meeresoberflächen-Temperaturen im Juli–August während feuchter minus trockener Jahre im randsaharischen Westafrika

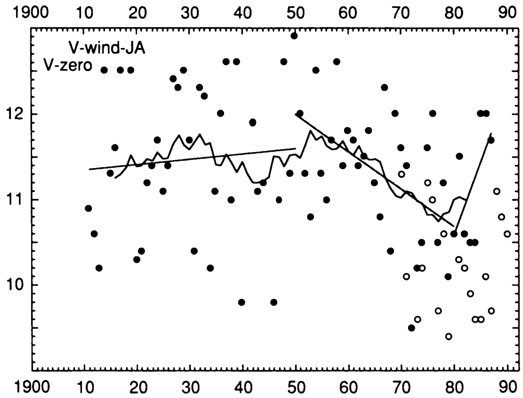

Fig. 6: Scatter plot of the latitude position of the wind confluence (zero meridional wind component) over the eastern tropical Atlantic (15–40° W) during July-August. Solid and open dots indicate the data sets with one-degree versus two-degree resolution
Source: Hastenrath 1990 a

Streudiagramm der Breitenlage der Windkonfluenz (meridionale Windkomponente = 0) über dem östlichen tropischen Atlantik (15–40° W) im Juli-August

Atlantic waters cooled and those of the South Atlantic and Western Indian Oceans warmed, most markedly at the height of the boreal summer rainy season in the Sahel; patterns in the North Atlantic being less distrinct during the winter. Figs. 7 and 4 thus indicate that the associations of SST and rainfall departures on the decadal time scale occurred in the same sense as shown above for the interannual time scale.

With this synthesis of earlier work on the interannual and decadal-scale variations of ocean thermal conditions and Sahel rainfall during 1948–83, inquiry will in section 4 be directed to the diverse climatic trends that have occurred in this century.

3 Data sources and analysis

The datasets used here include long-term ship observations of SST and surface wind in the tropical oceans and index series of the hydrometeorological conditions in Subsaharan West Africa.

Widely used is the rainfall index SAHEL compiled by Lamb (1985) from the April–October precipitation at 20 stations across Subsaharan West Africa. The series starts in 1941 and is continously being updated (Lamb a. Pepper 1991; P. Lamb, pers. commun. 1992). The domain represented by this index is indicated in Fig. 1, and a time series plot is displayed in Fig. 4. An alternative is offered by the measurements of the river discharge of the Senegal at Bakel beginning in 1903. The discharge values for the hydrological year May through April, here denoted as SENEGAL, are available in Faure a. Gac (1981) and the series was updated through the courtesy of ORSTOM, Montpellier, France. The Senegal river

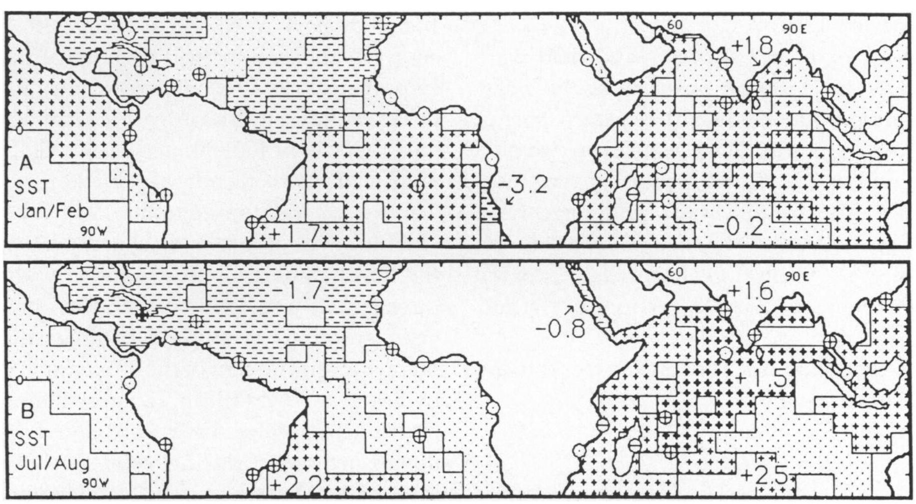

Fig. 7: Maps of linear trends of sea surface temperature in 1948–83. A = January-February, B = July-August. Enhanced symbols represent 5 % significance level, and dot raster indicates absolute trends below 6×10^{-3} °C per year. Numerical values are given in 10^{-2} °C per year for all significant trends and for the extreme values in the Atlantic and Indian Ocean domains, respectively
Source: Wolter a. Hastenrath 1989

Karte der linearen Trends der Meeresoberflächen-Temperaturen 1948–1983. A = Januar-Februar, B = Juli-August

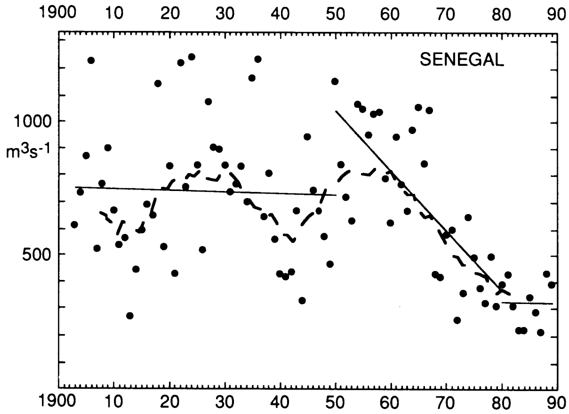

Fig. 8: Time series plot of hydrometeorological index series SENEGAL (ref. Fig. 1), in m^3s^{-1}. Heavy dots denote individual years, dashed line eleven-year running means, and solid line trends for the intervals 1901-50, 1950-80, 1980-90

Darstellung der Zeitreihen des hydrometeorologischen Index SENEGAL (Abfluß in m^3s^{-1})

catchment is entered in Fig. 1, and a time series plot is displayed in Fig. 8.

SST observations in the tropical oceans since the beginning of the century were taken from the "File 31" in BOTTOMLEY et al. (1990). Available by calendar months and in a five-degree-square spatial resolution, these were compacted into the domains NATL, SATL, and IND, as delineated in Fig. 1, for the bimonthly "seasons" March-April and July-August and over the period 1901-89.

Ship observations of the surface wind field were used to evaluate the latitude position of the near-equatorial wind confluence over the eastern part of the tropical North Atlantic. These stem from two data sources: data with a one-degree-square spatial resolution are available through 1987 and have been described in HASTENRATH a. LAMB (1977); a data set with a two-degree resolution has been updated beyond 1989 as part of COADS (WOODRUFF et al., 1987).

Time series were examined for linear trend using the least-squares fit equation

$$y = a + b \times t \qquad (1)$$

where b is the slope of the series with time t, and at its interception point with the ordinate. The formula is arrived at by a least squares fit of the time series with respect to time, obtaining not only the trend and interception point, but also the amount of variance accounted for by Eq. (1). Statistical significance is assessed by comparing the trend against the possibility of arriving at the same trend by chance if the real trend were equal to zero (SPIEGEL 1975, p. 289; OORT et al. 1987).

4 Regimes of climatic trends

As discussed in section 2 and illustrated in Figs. 4, 6 and 7, the time span from the late 1940's to the early 1980's has received some previous attention as an era during which the rainfall in Subsaharan Africa drastically declined (Fig. 4), in the large-scale context consistent with a concomitant southward shift of the near-equatorial wind confluence (Fig. 6), as well as a cooling of the tropical North Atlantic and a warming of the South Atlantic and Indian Oceans (Fig. 7). With this background, the present section shall explore the climatic evolution since the beginning of the century, with particular focus on developments during the most recent decade 1980-90. Explicitly, the regime of 1950-80 shall be compared to the first half of the century and the development since the early 1980's.

The pertinent observational evidence is presented in Figs. 8-11 and Table 1. While the precipitation index SAHEL (Fig. 4) compiled from raingauges starts only in 1941, the hydrometeorological conditions in the western part of the Subsaharan zone since the beginning of the century are effectively described by the discharge measurements of the Senegal river at Bakel (Figs. 1 a. 8). As for Figs. 10-11, the graph shows in addition to the individual annual values, the smoother curve of eleven year running means, and the trend lines, or linear least-square fit, for the intervals 1900-50, 1950-80, and 1980-90. The numerical values of these trends are further summarized in Table 1 (a). Compared to the 1950-80 regime, Fig. 4 exhibits overall larger discharge values throughout the first half of the century, albeit with considerable interannual and long-term variations. The eleven-year running mean curve suggests some cyclic behavior reminiscent of the 35-year periodity claimed by FAURE a. GAC (1981). In agreement with the other hydrometeorogical index presented in Fig. 4, the downward trend during 1950-80 did not continue into the 1980's, when in fact some opposite tendency is indicated. Of the three time spans distinguished in Table 1 (a) only for 1950-80 does the (strongly negative) trend reach conventional statistical significance.

Fig. 6 and Table 1 (b) illustrate the long-term variations in the latitude position of the near-equatorial

*Table 1: Linear trends during intervals 1901–50, 1950–80, and 1980–90**⁾

Lineare Trends für die Zeitintervalle 1901–50, 1950–80 und 1980–90

	1901–50	1950–80	1980–90
(a) Hydrometeorological indices			
SENEGAL	– 0.6	– 22.5**	+ 0.0
SAHEL	+ 0.04	– 0.06**	+ 0.05
(b) July–August wind confluence			
	+ 6	– 44**	+ 17
(c) July–August SST			
ΔNS	– 0.3	– 3.5**	– 8.5
NATL	+ 1.8**	– 1.8*	+ 5.7
SATL	+ 2.1**	+ 1.2	+ 14.2*
IND	+ 1.6**	+ 3.0**	+ 5.5
(d) March–April SST			
ΔANS	– 0.4	– 1.7	– 23.8**
NATL	+ 2.2**	– 1.4	– 2.5
SATL	+ 2.6**	+ 0.4	+ 16.3*
IND	+ 0.9	+ 1.5	+ 6.1
(e) PAC			
MA	– 0.4	– 0.0	– 6.9
JA	– 0.7	+ 0.3	+ 6.7

*⁾ One and two asterisks indicate significance at the 5 and 1% levels, respectively

(a) Hydrometeorological indices: SENEGAL river discharge in m^3s^{-1} yr^{-1}; SAHEL rainfall index, units yr^{-1} (approximately corresponding to 10^2 mm yr^{-1}/yr)
(b) Near-equatorial wind confluence during boreal summer, in 10^{-3} degrees of latitude North per year
(c) July–August sea surface temperature (SST) in domains NATL, SATL, IND, ref. Fig. 1. ΔNS is the difference of NATL minus SATL. In °C yr^{-1}
(d) March–April SST, as in (b)
(e) Equatorial Pacific (ref. Fig. 1) SST, PAC in March–April (MA) and July–August (JA), as for (b) and (c)

wind confluence at the July–August height of boreal summer. For most of the record the fine one-degree spatial resolution was available, as described in section 3; this is complemented by a coarser analysis for the more recent years. Apart from large year-to-year variations, long-term trends are of interest here. There is little indication of this for the first half of the century; most prominent being the marked southward shift during 1950–80 mentioned above. Fig. 6 and Table 1 (b) indicate a reversal of this trend during the most recent decade.

Fig. 9 (b–d) and Table 1 (c) examine the SST evolution at the July–August height of the boreal summer, separately for the tropical North and South Atlantic and the Indian Oceans. The thermal contrast between the tropical North and South Atlantic is also shown in Fig. 9 (a). For the 1950–80 time span, the three ocean domains (Fig. 9 (b–d), Table 1 (c)), exhibit the pattern familiar from Fig. 7, namely a cooling in the tropical North Atlantic contrasting with a warming in the South Atlantic and Indian Oceans; this opposition of temperature trends leads to a weakening of the thermal contrast across the Atlantic Equator (Fig. 9 (a), Table 1 (c)).

Turning to the first half of the century, all three ocean domains (Fig. 9 (b–d), Table 1 (b)), exhibit an apparent warming trend of several tenths of °C. As pointed out by FOLLAND et al. (1984) and WRIGHT (1986) and reviewed by WOLTER a. HASTENRATH (1989), a portion of this apparent temperature increase is to be attributed to changes in the practices of measuring SST, especially the conversion from the bucket to the injection methods, a transition largely completed by 1950 (FOLLAND et al. 1984, WRIGHT 1986). With this reservation, however, a substantial portion of the apparent warming trend over the first half of this century indicated in Fig. 9 (b–d) is to be regarded as real. This was followed during 1950–80 by further warming in the tropical South Atlantic and Indian Oceans, but by cooling in the North Atlantic

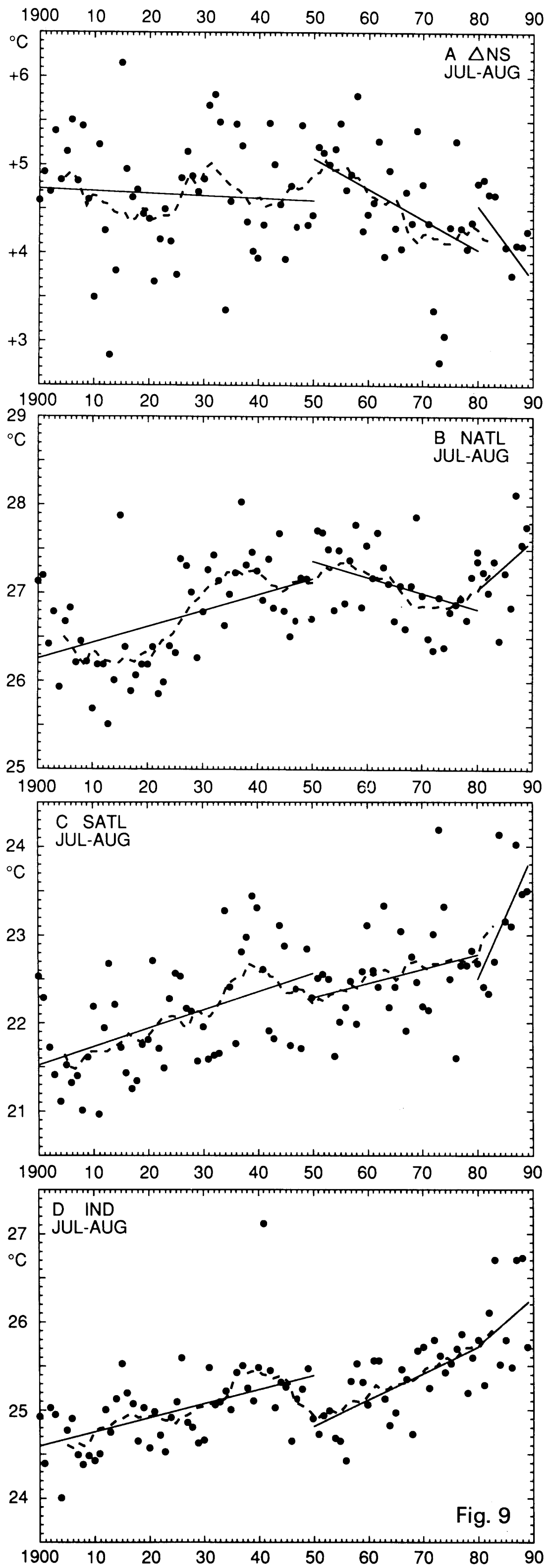
A ΔNS
JUL-AUG
B NATL
JUL-AUG
C SATL
JUL-AUG
D IND
JUL-AUG
°C

Fig. 9

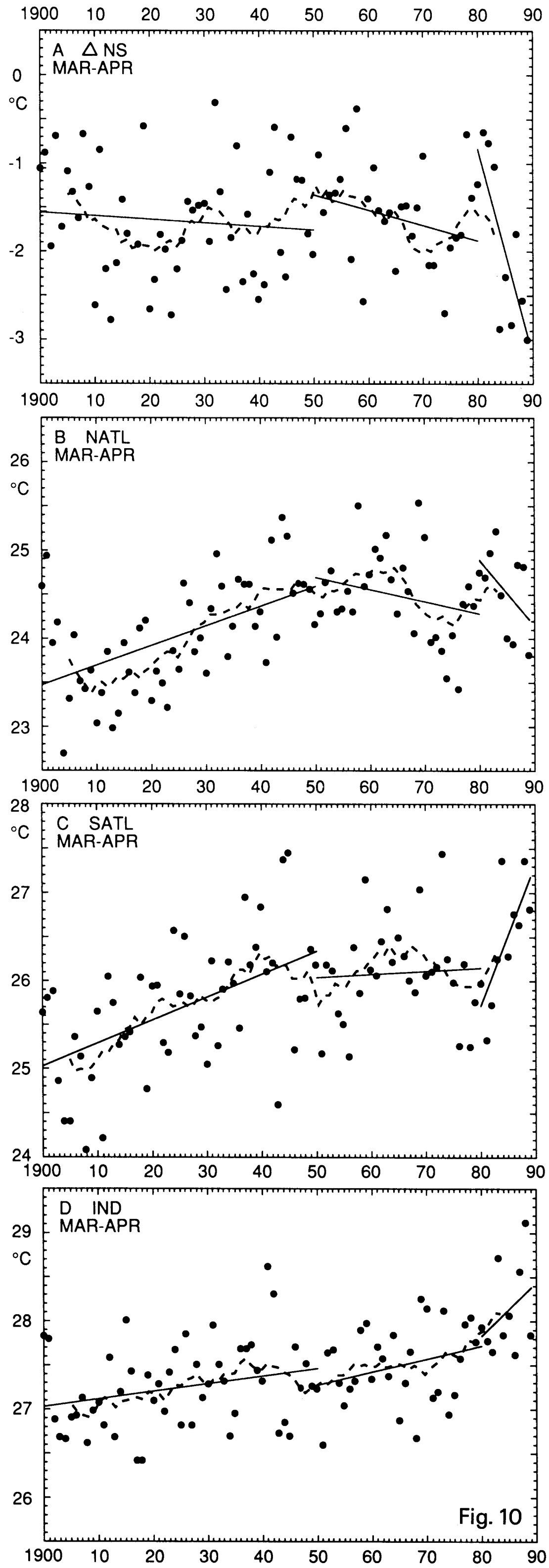
A ΔNS
MAR-APR
B NATL
MAR-APR
C SATL
MAR-APR
D IND
MAR-APR
°C

Fig. 10

(Fig. 9 (b–d), Table 1 (c)). In the process, the meridional SST contrast across the Atlantic Equator (Fig. 9 (a), Table 1 (c)), which had shown little systematic long-term change over the first half of the century, diminished markedly during 1950–80.

The evolution during the most recent decade 1980–90 is of particular interest. In the tropical South Atlantic and Indian Oceans, the warming trend apparent since the beginning of the century (or before) intensified; more importantly, the tropical North Atlantic changed from a cooling to a distinct warming trend, sharing this now with the other two ocean domains (Fig. 9 (b–d), Table 1 (c)). However, inasmuch as the tropical North Atlantic waters warmed at a lesser rate than those of the South Atlantic, the interhemispheric temperature contrast in the tropical Atlantic decreased further (Fig. 9 (a)).

To complement the above discussion for the height of the boreal summer, when weather activity and rainfall in the Sahel are concentrated, Fig. 10 and Table 1 (d) document the regimes of long-term changes at the opposing extreme of the annual cycle: for the tropical Atlantic sector, this is indeed March–April rather than January–February (HASTENRATH a. LAMB 1977). Fig. 10 and Table 1 (d) show much similarity with the boreal summer conditions (Fig. 9 and Table 1 (b)), but also remarkable differences. The first half of the century featured apparent warming trends in all three ocean domains also in March–April (Fig. 10 (b–d), Table 1 (d)), of a magnitude similar to those in July–August (Fig. 9 (b–d), Table 1 (d)).

Over the 1950–80 period, the March–April (Fig. 10 (c–d), Table 1 (c)) warming trends in the tropical South Atlantic and Indian Oceans were weaker than those of January–February (Fig. 10 (c–d), Table 1 (d)), while the North Atlantic experienced a weaker cooling trend in March–April (Fig. 10 (b), Table 1 (d)) than in January–February (Fig. 9 (b), Table 1 (c)). Accordingly, the interhemispheric SST contrast in the tropical Atlantic diminished less for March–April (Fig. 10 (a), Table 1 (d)) than for July–August (Fig. 9 (a), Table 1 (c)).

During the most recent decade 1980–90, the tropical South Atlantic and Indian Oceans experienced an accelerated warming rate (compared to 1901–50) for March–April (Fig. 10 (b–d), Table 1 (c)) as well as for January–February (Fig. 9 (b–d), Table 1 (c)). Most remarkable, however, is the tropical North Atlantic, where March–April (Fig. 10 (b), Table 1 (c)) did not share the warming trend at the July–August height of the boreal summer season (Fig. 9 (b), Table 1 (d)). As for July–August (Fig. 9 (a), Table 1 (c)), the interhemispheric SST contrast in the tropical Atlantic decreased further also in March–April (Fig. 10 (a), Table 1 (c)).

The SST history of the equatorial Pacific (Fig. 1) is presented in Fig. 11 and Table 1 (e). Little trends are apparent except for a warming over the most recent decade during July–August.

Fig. 9: Time series plots of July–August sea surface temperature indices, in °C. (ref. Fig. 1 for location of areas). A = ΔNS = difference of NATL minus SATL, B = NATL, C = SATL, D = IND. Symbols as for Fig. 8

Darstellung der Zeitreihen der Meeresoberflächen-Temperaturindizes für Juli–August (in °C)

Fig. 10: Time series plots of March–April sea surface temperature indices, in °C. (ref. Fig. 1 for location of areas). A = ΔNS = difference of NATL minus SATL, B = NATL, C = SATL, D = IND. Symbols as for Fig. 8

Darstellung der Zeitreihen der Meeresoberflächen-Temperaturindizes für März–April (in °C)

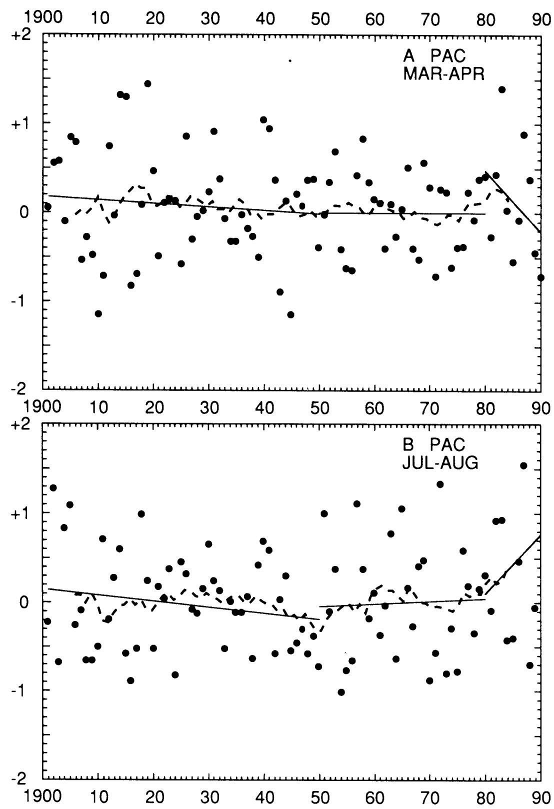

Fig. 11: Time series plots of sea surface temperature index PAC (ref. Fig. 1 for location of area). A = March–April, B = July–August. Symbols as for Fig. 8

Darstellung der Zeitreihen des Meeresoberflächen-Temperaturindex für den äquatorialen Pazifik. A = März–April, B = Juli–August

5 Conclusions

Widespread recent publicity has linked the „greenhouse effect" to the notion of a „global warming", usually implying a temperature increase at all places on Earth. More plausibly, one may wish to envisage alterations in the general circulation concomitant with diverse changes in regional temperature and climatic conditions. In this spirit, attention was here focused on Subsaharan West Africa which has experienced a sustained and drastic change of its climate and environment in recent decades, and the tropical Atlantic and Indian Oceans which in earlier work have been found to possess considerable affinity to extreme climatic events in the Sahel.

Three major regimes of climatic trends can be distinguished in this century, broadly spanning the periods 1900–50, 1950–80, and from 1980 onward. During the first half of the century, a warming is apparent in the tropical Atlantic and Indian Ocean regions examined here, that can only in part be attributed to systematic observational bias. Superimposed on this long-term trend, the tropical North Atlantic shows relative minima in the 1910's and 1940's, and maxima in the 1920's and 1950's, which broadly accompany quasi-cyclical long-term variations in the discharge of the Senegal River. It is over the decades 1950–80 that a progressively aggravating drought has struck the Sahel, unprecedented in its severity and persistence. It was accompanied by a southward shift of the near-equatorial wind confluence, cooling of the North Atlantic in the boreal summer, and a warming of the tropical South Atlantic and Indian Oceans – long-term evolutions consistent with the circulation anomaly patterns previously found characteristic of individual extreme events in the Sahel.

At variance with these climatic patterns established during 1950–80, is the evolution that is becoming apparent since 1980: The Sahel drought is showing a respite, concurrent with a northward shift of the near-equatorial wind confluence during boreal summer, and a change from cooling to warming in the summertime tropical North Atlantic, while the upward SST trend in the other tropical ocean regions appears further accelerated. In conjunction and in perspective with the problem of global change, these very recent developments emerging in the tropical Atlantic-African sector underline the need for sustained attention to changes in the various components of the climate system.

Acknowledgements

This paper is in memory of recurrent exchanges of thought with WILHELM LAUER on the climate and environment of the tropics, spread over three decades, and our hike to the glaciers of the Venezuelan Andes in 1978. The study was supported by U.S. National Science Foundation Grant ATM-9101097 and NOAA Grant NA26GPO88-01.

References

BHATT, U.: Circulation regimes of rainfall anomalies in the African-South Asian monsoon belt. In: J. Climate 2, 1989, 1133–1144.

BOTTOMLEY, M., FOLLAND, C. F., HSIUNG, J., NEWELL, R. E. a. PARKER, D. E.: Global ocean surface temperature atlas. Meteorological Office. Bracknell, UK, 1990.

DETTWILLER, J.: Note sur la structure du front intertropical boréal sur le Nord-Ouest de l'Afrique. In: La Météorologie 6, 1965, 337–347.

FAURE, H. a. GAC, J. Y.: Will the Sahelian drought end in 1985? In: Nature 291, 1981, 475–478.

FOLLAND, C. K., PALMER, T. N. a. PARKER, D. E.: Sahel rainfall and worldwide sea temperature. In: Nature 320, 1986, 602–607.

FOLLAND, C. K., PARKER, D. E. a. KATES, F. E.: Worldwide marine temperature fluctuations, 1856–1981. In: Nature 310, 1984, 670–673.

GERMAIN, H.: Météorologie dynamique et climatologie: applications au régime de pluies du Sénégal. ASECNA, Direction de l'Exploitation Météorologique. Dakar, Sénégal, 1968.

GORE, A.: Earth in the balance: ecology and the human spirit. Boston, New York, London 1992.

HASTENRATH, S.: On modes of tropical circulation and climate anomalies. In: J. Atmos. Sci. 35, 1978, 2223–2231.

– : Interannual variability and annual cycle: mechanisms of circulation and climate in the tropical Atlantic sector. In: Mon. Wea. Rev. 112, 1984, 1097–1107.

– : Decadal-scale changes of the circulation in the tropical Atlantic sector associated with Sahel drought. In: Int. J. Climatol. 10, 1990a, 459–472.

– : Third WMO Symposium on the meteorological aspects of tropical droughts with emphasis on long-range forecasting, April–May 1990, Niamey, Niger. In: WMO Bulletin 39, 1990b, 284–287.

– : Climate dynamics of the tropics. Dordrecht, Boston, London 1991.

HASTENRATH, S. a. KRUSS, P. D.: The dramatic retreat of Mount Kenya's glaciers 1963–87: greenhouse forcing. In: Annals Glaciol. 16, 1992, 127–133.

HASTENRATH, S. a. LAMB, P.: Climatic atlas of the tropical Atlantic and Eastern Pacific Oceans. University of Wisconsin Press 1977.

HOUGHTON, J. T., JENKINS, G. J. a. EPHRAUMS, J. J. (Eds.): Climate change, the IPCC scientific assessment. Cambridge 1990.

LAMB, P.: Case studies of tropical Atlantic surface circulation patterns during recent Sub-Saharan weather anomalies: 1967 and 1968. In: Mon. Wea. Rev. 106, 1978a, 482–491.

– : Large-scale tropical Atlantic circulation patterns associated with Subsaharan weather anomalies. In: Tellus 30, 1978b, 240–251.

– : Rainfall in Subsaharan West Africa during 1941–83. In: Zeitschrift für Gletscherkunde und Glazialgeologie 21, 1985, 131–139.

LAMB, P. a. PEPPLER, R. A.: West Africa. In: GLANTZ, M. H., KATZ, R. W. a. NICHOLLS, N. (Eds.): Teleconnections: linkages between ENSO, worldwide climate anomalies, and societal impacts. Cambridge 1991, 121–189.

OORT, A. H., PAN, Y. H., REYNOLDS, R. W. a. ROPELEWSKI, C. F.: Historical trends in the surface temperature over the oceans based on the COADS. In: Climate Dynamics 2, 1987, 29–38.

SPIEGEL, M. R.: Probability and statistics. New York 1975.

WOLTER, K. a. HASTENRATH, S.: Annual cycle and long-term trends of circulation and climate variability over the tropical oceans. In: J. Climate 2, 1989, 1329–1351.

WOODRUFF, S. D., SLUTZ, R. J., JENNE, R. L. a. STEURER, P. M.: A comprehensive ocean-atmosphere data set. In: Bull. Amer. Meteor. Soc. 68, 1987, 1239–1250.

WRIGHT, P. B.: Problems in the use of ship observations for the study of interdecadal climate changes. In: Mon. Wea. Rev. 114, 1986, 1028–1034.